

Pseudo-gradient algorithms for forecasting and filtering cylindrical images

V.R. Krasheninnikov¹, Yu.E. Kuvayskova¹, O.E. Malenova¹, A.U. Subbotin¹

¹Ulyanovsk State Technical University, Severny Venets street 32 , Ulyanovsk, Russia, 432027

Abstract. Currently, most of the image processing works deal with images defined on rectangular two-dimensional grids or grids of higher dimension. In some practical situations, images are set on a cylinder. For example, images of a section of a pipeline, a blood vessel, parts during turning, etc. The peculiarity of the domain for specifying such images requires its consideration in their models and processing algorithms. In the present work, autoregressive models of cylindrical images are considered, expressions of the correlation function depending on the autoregression parameters are given. To represent heterogeneous images with random heterogeneities, «doubly stochastic» models are used in which one or more images control the parameters of the resulting image. Note that the spiral scan of a cylindrical image can be considered as a quasiperiodic process due to the correlation of image lines. For example, voiced speech sounds and musical tones. The scans of two or more correlated cylindrical images can serve as a model of a system of correlated quasiperiodic processes. Pseudogradient algorithms for filtering and predicting images and processes and identifying their models are proposed. The conducted statistical modeling showed that these algorithms are close in efficiency to the optimal algorithms constructed with known values of the parameters of the processed data.

1. Introduction

Currently, the vast majority of image processing works deal with images defined on rectangular two-dimensional grids or grids of higher dimension [1-7]. There are much fewer works on images defined on the sphere and other curved surfaces, for example, [8-11]. However, sometimes images are set on the cylinder. For example, images of a pipeline, a blood vessel, a part during turning, a tree trunk, etc. Traditional models of rectangular images can be used to model only small sections of such images, and to describe the entire image, the model would have to be very complicated by breaking the cylinder into many sections. In this paper, we use a single autoregressive model of the entire cylindrical image. The pseudo-gradient adaptive algorithms for their prediction and filtering are constructed based on these image models.

2. Models of random fields on a cylinder

We first consider the well-known autoregressive model of a flat image [6]:

$$x_{k,l} = a x_{k,l-1} + b x_{k-1,l} - a b x_{k-1,l-1} + \beta \xi_{k,l} \quad (1)$$

where k is the number of the row; l is the number of the column; $\xi_{k,l}$ are independent standard random variables.

Figure 1 (a) shows an example of simulating an image using this model. Figure 2 shows a graph of several rows of such an image, separated by vertical lines.

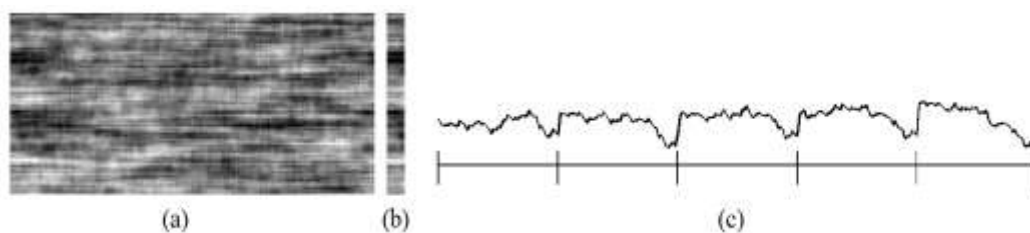


Figure 1. Model simulated image (1): (a) scan image, (b) first columns, (c) graph of adjacent image lines.

Parameters a , b affect the horizontal and vertical correlations of the image, respectively; β affects the dispersion of the image. The generated image has zero mean and covariance function (CF)

$$V(m, n) = M[x_{k,l} x_{k+m, l+n}] = \frac{\beta^2 a^{|m|} b^{|n|}}{(1-a^2)(1-b^2)},$$

the graph of which is shown in figure 2.



Figure 2. CF graph of the model (1).

Correlation between image elements decreases along rows and columns. Therefore, the elements of this image located at the beginning and end of the row are weakly dependent. When connecting the image into the cylinder (between figure 1 (a) and 1 (b)), there will be a large jump in brightness at the junction that is not characteristic of the image on the cylinder. The adjacent rows of the rectangular image with $b \approx 1$ have a high correlation, therefore, when combining the rows into a sequence, we can obtain a model of a quasiperiodic process. However, the beginning and end of each row, being at a considerable distance from each other, are practically independent of each other, so there will be sharp jumps at the junction of the quasiperiods of the process, which are unusual for relatively continuous processes (figure 1 (c)).

Thus, rectangular images do not give acceptable representations of cylindrical images and quasiperiodic processes. In this paper, for this purpose, we use images defined on a cylinder, the values of which along the spiral do not have undesirable sharp jumps.

3. Autoregressive model of a homogeneous cylindrical image

Consider a spiral grid on the cylinder (figure 3 (a)). Rows of this grid are turns of a cylindrical spiral. The turns of this image can also be considered as closed circles on the cylinder with the same numbering (figure 1 (b)). To describe the image defined on a cylindrical grid, we use an analog of the autoregressive model (1), where k is a spiral turn number and l is a node number ($l=0, \dots, T$), T is the period, i.e. the number of points in one turn [9, 10]. This model can be represented in equivalent form as a scan of the image along a spiral:

$$x_n = a x_{n-1} + a x_{n-T} - ab x_{n-T-1} + \beta \xi_n \quad (2)$$

where $n=kT+l$ is end-to-end image point number. A cross-section of the image obtained using this model is shown in figure 4.

A characteristic feature of CF (3) is its continuity at the junction of periods, in contrast to figure 2. The image in figure 4 is also continuous along the cut line, which is noticeable in the first few columns attached to this image. As a result, the process described by model (2), that is, the scan of the cylindrical image in a spiral, does not have sharp jumps at the junction of periods (figure 6). The examples of simulating cylindrical images at various values of the model parameters (2) are shown in figure 7.

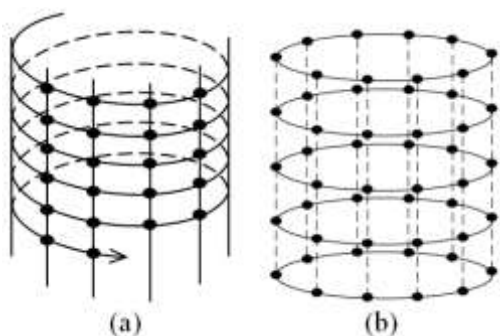


Figure 3. Grids: (a) cylindrical, (b) circular.

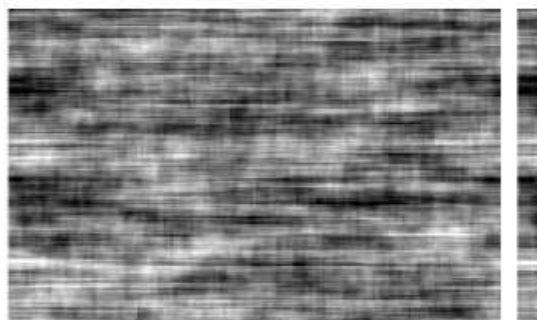


Figure 4. Section of a cylindrical image.

It can be shown that the CF of model (2) has the form:

$$V(n) = \beta^2 \left(\frac{1}{(1-b^2)T} \sum_{k=0}^{T-1} \frac{z_k}{(1-az_k)(z_k-a)} z_k^n + \frac{s}{(1-a^2)(1-bs)(s-b)} \rho^n \right), \quad (3)$$

where $z_k = \sqrt[T]{be} e^{i\frac{2\pi k}{T}}$ and $s = a^T$. The graph view of such a CF is shown in figure 5.

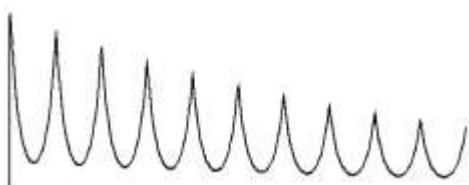


Figure 5. Graph of CF process model (2).

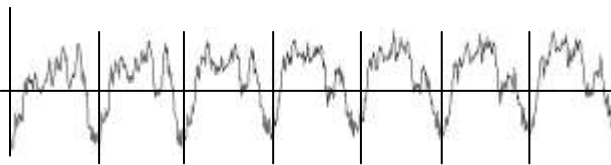


Figure 6. Schedule of a simulation of a process by a model (2).

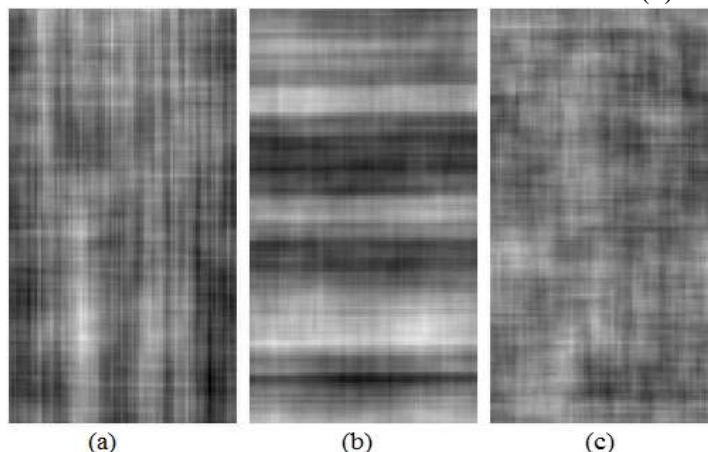


Figure 7. Simulated images on a cylinder: (a) $a = 0.95, b = 0.99$; (b) $a = 0.99, b = 0.95$; (c) $a = b = 0.95$

4. Autoregressive model of an inhomogeneous cylindrical image

The images generated by models (1) and (2) are homogeneous, which limits the scope of their application, since many images and signals have significant and random heterogeneity. In [12], it was proposed to represent the heterogeneity of images in the form of «doubly stochastic» model on rectangular grids. In this view, several common «control» images set random parameters for a «managed» resulting image. The heterogeneity of the resulting image is determined by the local features of the control images.

To represent inhomogeneous cylindrical images [13], we apply the doubly stochastic model similar to those considered in [12]. To do this, let us take two images $U = \{u_n\}$ and $V = \{v_n\}$ defined by

models (2) with some of their parameter values as control images. The managed image X is also set by the model (2) with variable parameters $a_n = u_n, b_n = v_n$.

Figure 8 shows an example of applying this model to simulate an image on a cylinder. There is only one control image ($U=V$) which is shown in figure 8 (a). The final image in figure 8 (b) has a pronounced heterogeneity caused precisely by the variability of the parameters of model (2). The dark areas of figure 8 (a) correspond to small values a_n and b_n , therefore, at these places figure 8 (b) is less correlated.

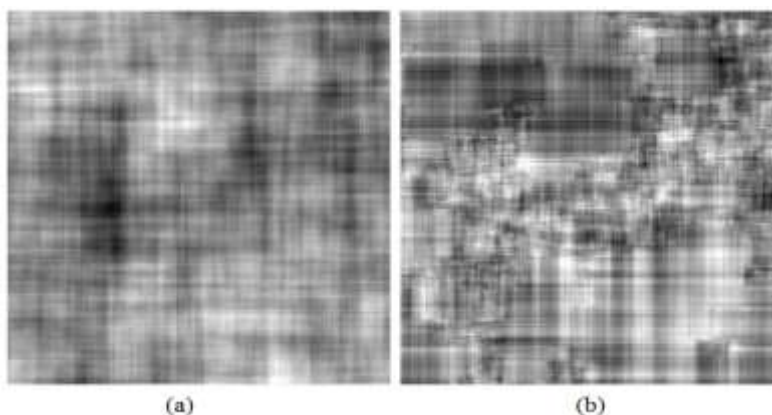


Figure 8. Simulation of double stochastic image on a cylinder: a) control image, b) final image.

Figure 9 shows graphs of two segments of a quasiperiodic signal simulated using the described doubly stochastic model with period $T=25$. The quasiperiods are separated by vertical lines. Parameters a_n and b_n change with time, so the correlation properties of the final process also change. The upper graph corresponds to large values of these parameters, therefore, the process is close to purely periodic. At small values of the parameters, the periodicity is weaker (lower graph).

Thus, the described double-stochastic models of cylindrical images can serve as the basis for modeling and simulating quasiperiodic processes with a wide spectrum of non-stationarity by an appropriate set of model parameters.

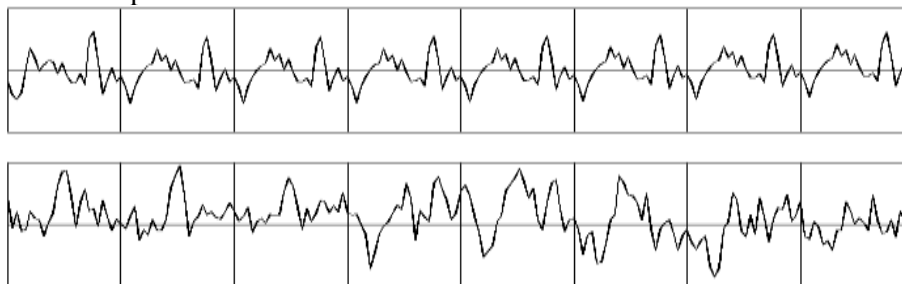


Figure 9. Plots of simulated quasiperiodic process.

5. Model identification, prediction and filtering of a cylindrical image

Let an informative cylindrical image $X = \{x_n\}$ be given by model (2) and its observations $Z = \{z_n\}$ have the form:

$$z_n = x_n + \theta_n, \quad (4)$$

where the noise $\Theta = \{\theta_n\}$ is the set of independent Gaussian random variables with zero mean and variance σ_θ^2 . It is required to build a forecast \tilde{x}_n of the next value of x_n from observations $\{z_i, i < n\}$ and to estimate \hat{x}_n (filtering) from the observations $\{z_i, i \leq n\}$. To solve this problem with unknown parameters a, b and σ_θ^2 we use the adaptive pseudogradient version of the Kalman filter [9, 13, 14]:

$$\hat{x}_n = \tilde{x}_n + s_n(z_n - \tilde{x}_n) = \tilde{x}_n + s_n \Delta_n, \quad \tilde{x}_n = a_n \hat{x}_{n-1} + b_n \hat{x}_{n-T} - a_n b_n \hat{x}_{n-T-1}, \quad (5)$$

where the vector of parameters $\bar{a}_n = (a_n, b_n, s_n)$ is calculated using the procedure:

$$\begin{aligned} a_{n+1} &= a_n + h \cdot \text{sign}\{\Delta_n(\hat{x}_n - a_n \hat{x}_{n-T-1})\}, \\ b_{n+1} &= b_n + h \cdot \text{sign}\{\Delta_n(\hat{x}_{n-T} - a_n \hat{x}_{n-T-1})\}, \\ s_{n+1} &= s_n + h \cdot \text{sign}\{\Delta_n \Delta_{n-1}\}. \end{aligned} \quad (6)$$

The components of the vector $\bar{a}_n = (a_n, b_n, s_n)$ are forcibly limited to values from 0 to 1 for more stable operation of the algorithm with step h .

Figure 10 shows an example of filtering of the inhomogeneous cylindrical image with unit variance and sharply changing autoregression parameters. ($a=0.95, b=0.5$ or vice versa $a=0.5, b=0.95$). Figure 10 (a) shows an informative image, figure 10 (b) shows its noisy observation with $\sigma_\theta^2 = 1$, and figure 10 (c) shows the result of filtering. It is noticeable that on the first few rows (turns) the filtering errors are large, since procedure (6) takes some time to optimize the filtering parameters.

In particular, it follows from figure 11 (d) that there is an optimal value of h , near which the filtering accuracy varies slightly, so one can use $h=0.001$.

Note that the problem is greatly simplified if you only need to evaluate the parameters of model (2) without the noise. Then instead of two equations (5) there is only one

$$\tilde{x}_n = a_n x_{n-1} + b_n x_{n-T} - a_n b_n x_{n-T-1} \quad (7)$$

and in the filtering procedure (6) only the first two equations remain.

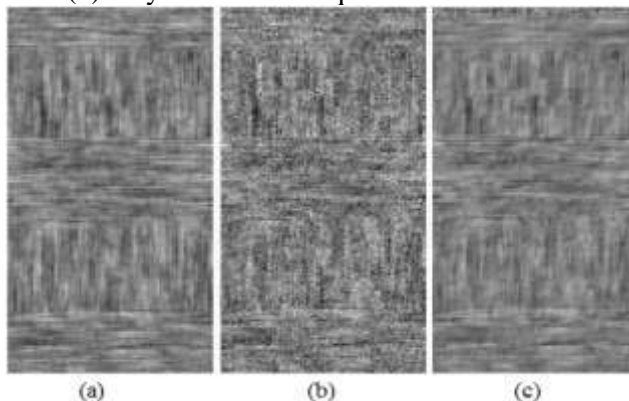


Figure 10. An example of an inhomogeneous image filtering: (a) an informative image; (b) noisy image; (c) result of filtration.

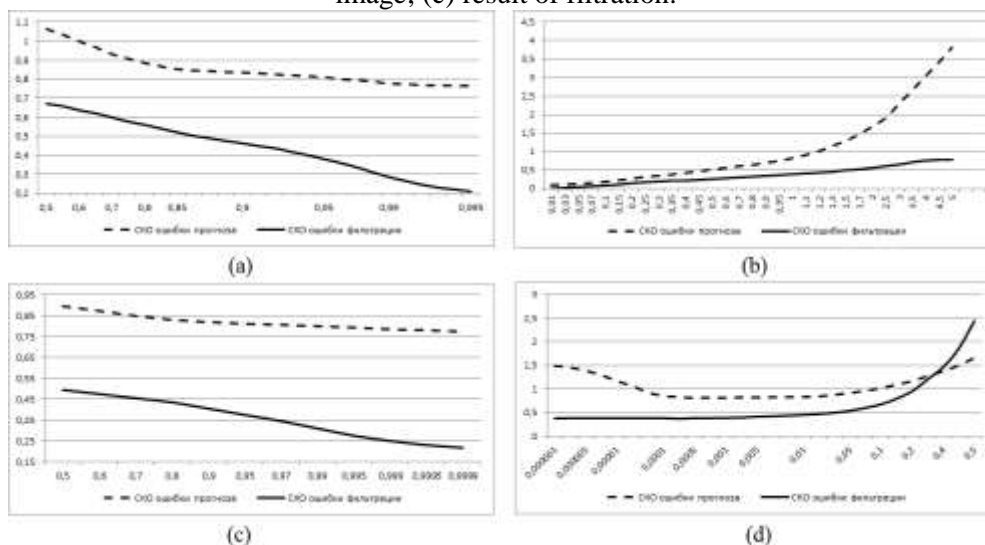


Figure 11. Graphs of the dependence of the standard deviation of forecast and filtering errors on the parameters of the informative image model and noise: (a) on the general correlation of the image ($a=b$); (b) on the standard deviation of noise σ_θ at $a=b=0.95$; (c) on the correlation a of the image along the row at $b=0.95, \sigma_\theta^2 = 1$; (d) on the step h of the procedure (6).

Figure 11 shows graphs of the dependence of the standard deviation SD of forecasting and filtering errors on the parameters of the informative image model and noise, and on the value of step h of procedure (5). These results were obtained by statistical modeling at $T=100$.

6. Conclusions

Autoregressive models of cylindrical images are considered in the paper. Correlation function expressions are given depending on autoregression parameters. To represent heterogeneous images with random heterogeneities, doubly stochastic models are used in which one or more images control the parameters of the resulting image. The spiral scan of a cylindrical image can be considered as a model of a quasiperiodic process. The paper proposes pseudo-gradient model identification algorithms. To identify the model, filtering and predicting images, adaptive pseudo-gradient algorithms are proposed. Examples of the application of these algorithms are provided.

7. Acknowledgments

The reported study was funded by the RFBR, project number 20-01-00613.

8. References

- [1] Soifer, V.A. Computer image processing. Part I: Basic concepts and theory / V.A. Soifer, S.B. Popov, V.V. Mysnikov, V.V. Sergeev // VDM Verlag Dr. Muller, 2009. – 300 p.
- [2] Myasnikov, V.V. Description of images using a configuration equivalence relation / V.V. Myasnikov // Computer Optics. – 2018. – Vol. 42(6). – P. 998-1007. DOI: 10.18287/2412-6179-2018-42-6-998-1007.
- [3] Shirokanev, A.S. Investigation of algorithms for coagulate arrangement in fundus images / A.S. Shirokanev, D.V. Kirsh, N.Yu. Ilyasova, A.V. Kupriyanov // Computer Optics. – 2018. – Vol. 42(4). – P. 712-721. DOI: 10.18287/2412-6179-2018-42-4-712-721.
- [4] Vizilter, Y.V. Morphological image analysis for computer vision applications / Y.V. Vizilter, Y.P. Pyt'ev, A.I. Chulichkov, L.M. Mestetskiy // Computer vision in control systems-1, Intelligent systems reference library 73 – Springer international publishing, 2015. – P. 9-58.
- [5] Gonzalez, R.C. Digital image processing / R.C. Gonzalez, R.E. Woods // Prentice-Hall, New York, 2017.
- [6] Habibi, A. Two-dimensional Bayesian estimate of images / A. Habibi // Proc IEEE. – 1972. – Vol. 60(7). – P. 878-883.
- [7] Woods, J.W. Two-dimensional Kalman filtering / J.W. Woods // Topics in Applied Physic. – 1981. – Vol. 42. – P. 11-64.
- [8] Shalygin, A.S. Applied methods of statistical modeling / A.S. Shalygin, Y.I. Palagin // Mechanical engineering, American society of mechanical engineers, 1986.
- [9] Krasheninnikov, V.R. Multidimensional image models and processing / V.R. Krasheninnikov, K.K. Vasil'ev // Computer Vision in Control Systems-3 Intelligent Systems Reference Library 135 Springer International Publishing Switzerland, 2018. – P. 11-64.
- [10] Krasheninnikov, V.R. Spiral autoregressive model of a quasi-periodic signal / V.R. Krasheninnikov, D.V. Kalinov, Yu.G. Pankratov // Pat Rec Im An. – 2001. – Vol. 8(1). – P. 211-213.
- [11] Krasheninnikov, V.R. Autoregressive models of random fields on the circle / V.R. Krasheninnikov, Yu.E. Kuvayskova, A.U. Subbotin // Journal of Physics: Conference Series, Image processing and earth remote sensing. – Vol. 1368 – 2019. – P. 032004
- [12] Vasil'ev, K.K. Doubly stochastic models of images / K.K. Vasil'ev, V.E. Dement'ev, N.A. Andriyanov // Pat Rec Im An. – 2015. – Vol. 25(1). – P. 105-110.
- [13] Dement'ev, V.E. Representation and processing of spatially heterogeneous images and image sequences / V.E. Dement'ev, V.R. Krasheninnikov, K.K. Vasil'ev // Computer Vision in Control Systems-5. Intelligent systems reference library 175 – Springer International Publishing, 2020. – P. 53-97.
- [14] Polyak, B.T. Optimal pseudogradient adaptation procedure/ B.T. Polyak, Ya.Z. Tsypkin // Automation and remote control. – 1980. – Vol. 8. – P. 74-84.